

Weierstraß-Institut für Angewandte Analysis und Stochastik

im Forschungsverbund Berlin e.V.

Preprint

ISSN 0946 – 8633

Mode transitions in distributed-feedback tapered master-oscillator power-amplifier

Mindaugas Radziunas¹, Vasile Z. Tronciu¹, Uwe Bandelow¹, Mark

Lichtner¹, Martin Spreemann², Hans Wenzel²

submitted: 29 September 2008

¹ Weierstraß-Institut
für Angewandte Analysis und Stochastik
Mohrenstrasse 39
D – 10117 Berlin
Germany
E-Mail: radziuna@wias-berlin.de,
tronciu@wias-berlin.de,
bandelow@wias-berlin.de,
lichtner@wias-berlin.de

² Ferdinand Braun Institut
für Höchstfrequenztechnik
Gustav-Kirchhoff-Str. 4
Einsteinufer 37
D – 12489 Berlin
Germany
E-Mail: martin.spreemann@fbh-berlin.de,
hans.wenzel@fbh-berlin.de

No. 1366
Berlin 2008



2000 *Mathematics Subject Classification.* 35Q60, 37L15.

Key words and phrases. master oscillator, power amplifier, taper, longitudinal mode analysis.

2006 *Physics and Astronomy Classification Scheme.* 42.55.Px, 42.65.Sf.
Supported by the DFG Research Center MATHEON "Mathematics for key technologies".

Edited by
Weierstraß-Institut für Angewandte Analysis und Stochastik (WIAS)
Mohrenstraße 39
10117 Berlin
Germany

Fax: + 49 30 2044975
E-Mail: preprint@wias-berlin.de
World Wide Web: <http://www.wias-berlin.de/>

Abstract

Theoretical and experimental investigations have been carried out to study the spectral and spatial behavior of monolithically integrated distributed-feedback tapered master-oscillators power-amplifiers emitting around 973 nm. Introduction of self and cross heating effects and the analysis of longitudinal optical modes allows us to explain experimental results. The results show a good qualitative agreement between measured and calculated characteristics.

1 Introduction

During recent years, compact lasers emitting single-frequency, diffraction limited continuous-wave (CW) beams at an optical power of several Watts have received considerable attention regarding several applications, such as frequency conversion, free-space communications, and pumping of fiber lasers and fiber amplifiers. Conventional narrow stripe or broad area semiconductor lasers do not meet these requirements, either due to the limited output power or the poor beam quality and wavelength stability. A device which is capable to maintain a good beam quality and wavelength stability in the Watt range is the monolithically integrated master-oscillator power-amplifier (MOPA), where either a distributed Bragg reflector (DBR) laser [1] or a distributed feedback (DFB) laser [2] and a flared (or tapered) gain-region amplifier are combined on a single chip. Recently, a DBR tapered MOPA, which emits a CW power of more than 10 W at 977 nm in a nearly diffraction limited beam and narrow spectral bandwidth of 40 pm, has been demonstrated [3]. In this paper we consider a monolithically integrated DFB tapered MOPA emitting around 973 nm. It is schematically shown in Fig. 1 and has been discussed in [4]. Different states can be observed in such devices when tuning injection currents in the MO and PA sections. In order to understand the origin of different instabilities and transitions between different states we analyze and simulate a mathematical model based on traveling wave equations which are coupled to a diffusion equation for the excess carrier density and an equation for gain dispersion [5, 6, 7]. In addition, we describe heating effects by a linear nonlocal dependence of the refractive index and the gain peak on the inhomogeneous injection current [4]. To resolve long transients and to perform a parameter continuation of this large scale system in reasonable time we have used high performance parallel distributed computing algorithms [8]. Our present study is based on former observations and analysis of longitudinal modes [9], their dynamics in narrow waveguide edge-emitting multisection lasers [10] and modeling of lasers with an external optical feedback [11]. Due to the residual field reflectivity at the PA facet, the MOPA device can be considered as a (DFB) laser with an optical feedback [10, 11]. The injection currents imply self- and cross- heating affecting the refractive indices of the PA and MO regions and thereby tune the relative optical phases. This phase tuning is responsible for the transitions between modes, observable both in optical experiments and in simulations.

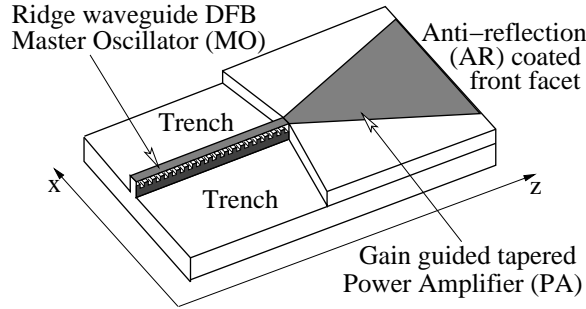


Figure 1: Schematic view of DFB tapered MOPA.

The paper is organized as follows. In Section 2 we introduce a short description of the laser device and present experimental characteristics of the MOPA. Section 3 gives a brief description of the model used for simulation of the MOPA device and shows simulation results. By performing a mode analysis of a simplified longitudinal model in Section 4 we explain some experimental observations. Finally, conclusions are drawn in Section 5.

2 Experimental characteristics of the MOPA device

Figure 1 shows the structure of the MOPA device that has been considered; it consists of an index guided DFB ridge-waveguide (RW) laser and a gain-guided tapered amplifier. Ridge width and effective-index step given by an etch depth are $2.5 \mu\text{m}$ and 0.004 , respectively. Both regions are separately contacted and can be driven independently. The coupling coefficient of the grating is about 2.5 cm^{-1} . Both facets are anti-reflection coated with a residual reflectivity of $R \approx 10^{-3}$. The lengths of the MO and the PA are 2 mm each. The PA has a total flare angle of 6° .

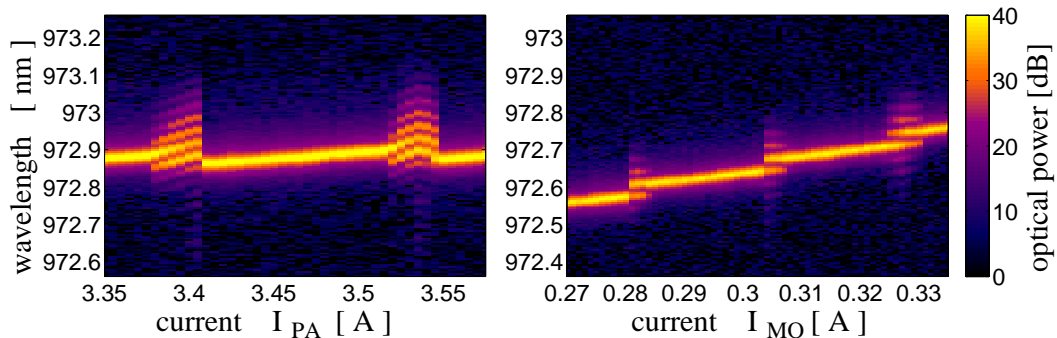


Figure 2: Mapping of measured optical spectra. Left: $I_{MO} = 0.35 \text{ A}$. Right: $I_{PA} = 2 \text{ A}$.

Figure 2 shows optical spectra measured under CW conditions at room temperature with increasing injection currents. We note that no significant differences (hysteresis) were found when injected currents were decreased. The diagrams show a basic

red shift of the lasing wavelength with increasing injected current as well as periodic changes of the lasing modes. During the exchange of modes a multimode mode-beating type pulsations with a frequency of about 10 GHz have been observed. This pulsation frequency corresponds to the field roundtrip time or mode separation in the compound laser cavity. Correlated with the mode jumps one observes small power fluctuations [4].

3 Mathematical model and simulation results

To simulate the dynamics of the MOPA device we use a Traveling Wave model [4, 5, 6, 7], which is given by the following model equations for the complex slowly varying amplitudes of the counterpropagating optical fields u^\pm :

$$\partial_t u^\pm + \frac{iv_g}{2k_0\bar{n}} \partial_{xx} u^\pm = v_g \left[(\mp \partial_z - i\beta(N(x, z, t))) u^\pm - i\kappa u^\mp \right]. \quad (1)$$

The wave equation (1) is coupled to an ordinary differential equation for the induced polarization and a parabolic diffusion equation for the real excess carrier density $N = N(x, z, t)$ with reflecting boundary conditions for the optical fields at both facets of the laser. For a detailed description of the full model we refer to [4, 8]. The model takes into account parameter distributions in longitudinal (z) and lateral (x) dimensions (see Fig. 1), while all quantities are averaged along the vertical dimension using the effective index method. We need to consider in more detail the thermal detuning δ_T due to heating contained in the full detuning

$$\delta(x, z, N, I) = \Re(\beta) = \delta_0(x, z) + \delta_n(x, z, N) + \delta_T(x, z, I),$$

where β is the complex propagation factor in (1), $\delta_0(x, z)$ is a built-in variation of the dielectric function, independent of the carrier density N and the temperature T , whereas δ_n and δ_T represent the dependence of the effective refractive index on N and heating due to current injection, respectively. We put the parametric dependencies:

$$\begin{aligned} \delta_T(x, z, I)|_{(x,z) \in MO} &= \delta_{T,MO} = \frac{k_0 n_g}{\lambda_0} \left(C_{T,MO}^{MO} I_{MO} + C_{T,MO}^{PA} I_{PA} \right), \\ \delta_T(x, z, I)|_{(x,z) \in PA} &= \delta_{T,PA} = \frac{k_0 n_g}{\lambda_0} \left(C_{T,PA}^{MO} I_{MO} + C_{T,PA}^{PA} I_{PA} \right), \\ \delta_T(x, z, I)|_{(x,z) \notin \{PA, MO\}} &= 0, \end{aligned} \quad (2)$$

where I_{MO} and I_{PA} denote the currents injected to the MO and PA, respectively, and C_T is a real 2×2 matrix describing local and nonlocal crosstalk thermal effects.

Model parameters used for simulations are similar to those in [4], where front reflectivities, gain and absorption needed to be adjusted. Figure 3 shows numerical calculations of optical spectra versus injection currents similar to that of Fig. 2. Both experiments and theoretical calculations are in good qualitative agreement. A proper estimation of the matrix C_T (see discussion in the next section) results in the same basic red shifts and periodicity of mode jumps with increase of the

injection currents. The regions of non-stationary behavior are characterized by multiple peaks of the optical spectra. These regions have a similar size in both theory and experiments. The peak separation corresponds to the spectral distance between compound cavity modes and is an indication of mode-beating pulsations. Compared

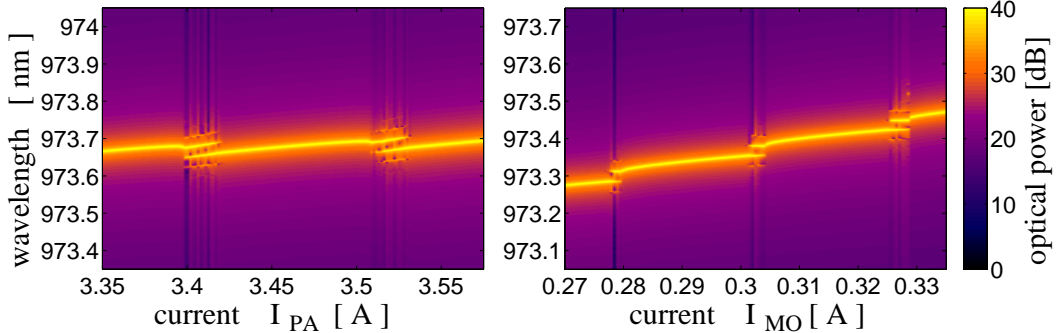


Figure 3: Simulated mapping of optical spectra. Left: $I_{MO} = 0.35$ A. Right: $I_{PA} = 2$ A.

to the short 1d laser discussed in [10] our long MOPA shows a more complicated dynamical behavior correlated with power fluctuations. Dynamical effects now depend more sensitive on model parameters. All of them have in common the basic mode switching behavior which we explain in Section 4. Investigations of the rich dynamical behavior will be subject to future work.

4 Mode analysis

In our previous paper [4] we have already stated, that the experimentally observed mode transitions can be explained by the nonvanishing field reflectivity at the PA front facet and thermally induced index changes. In this case the whole MOPA works as a compound cavity, where the PA section acts as an active feedback section. We now show how the observed mode transitions in Figs. 2 and 3 can be qualitatively explained by the mode analysis [9] corresponding to a simplified longitudinal TW model which neglects field diffraction and carrier diffusion, and simply treats the tapered PA part as a narrow stripe amplifier. In order to increase the optical feedback into the MO part of the device and to generate mode-beating pulsations we have to use a higher injection density within the amplifier together with a higher field reflectivity at the amplifier facet, compared to the 2d model parameters used in [4].

For any fixed carrier distribution $N(z)$ the partial differential operator on the right hand side of the field equations (1) gives rise to a spectral problem. The optical compound cavity modes correspond to eigenvalues (complex frequencies) and eigenfunctions of this spectral problem. The real part of an eigenvalue is the optical angular frequency and the imaginary part is the damping of the mode. According to this mode analysis, the optical fields can be represented as a superposition

of the eigenfunctions [12], which are slowly changing with variation of the carrier distribution $N(z)$.

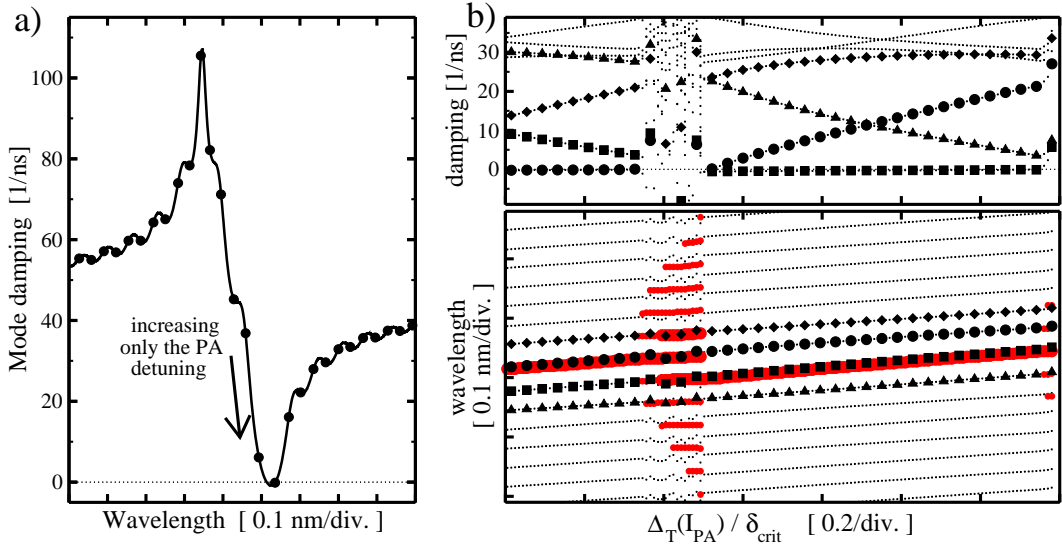


Figure 4: a): Calculated optical mode spectra at fixed stationary state. Bullets: complex mode frequencies. The eigenvalues follow the curve when increasing the full detuning δ_{PA} . b): Mode shift with increasing I_{PA} . Abscissa axis: scaled thermal detuning difference Δ_T . Dotted curves: damping (top) and wavelengths (bottom) of twenty neighboring modes. The four most important modes with lowest damping are indicated by black symbols. Thick and thin red (grey) in the lower panel represent the positions of the dominant peaks in optical spectra suppressed by ≤ 10 dB or ≤ 40 dB, respectively.

In Fig. 4a) we show the dependence of the eigenvalues on the detuning δ_{PA} in the PA section. First, we have integrated the longitudinal model equations to find some stationary state with certain spatial distribution of carriers $N(z)$. The corresponding eigenvalues of the related spectral problem are represented by the bullets in this figure. The eigenvalue with zero damping corresponds to the mode which determines the computed stationary state. In the next step we freeze the distribution $N(z)$ and increase the full detuning δ_{PA} in the PA section. The eigenvalues follow the curve according to the direction shown in the figure. They are replacing their next neighbor after this detuning is increased exactly by the critical value $\delta_{crit} = \frac{\pi}{l_{PA}}$, which corresponds to the frequency distance of two adjacent cold cavity Fabry-Perot modes in the amplifier section (l_{PA} denotes the length of the PA).

Due to cross-heating effects the full detuning δ_{MO} and $\delta_{PA} = \delta_{MO} + \Delta$ in both sections are increasing simultaneously. This increase implies the following two effects on the computed mode spectra. First, the increase of δ_{MO} causes a red shift of the whole curve in Fig. 4a). Second, the changing detuning difference Δ implies a simultaneous motion of the eigenvalues along this curve. The first of these effects in Figs. 2 and 3 governs the general (averaged) red shift, while the periodic mode exchange in these figures is due to the δ_{crit} -periodic change of the detuning difference Δ .

In Fig. 4b) we show changes of eigenvalues with increasing injection I_{PA} . Actually, on the abscissa axis we show the *thermal* detuning difference $\Delta_T = \delta_{T,PA} - \delta_{T,MO}$ which is linearly increasing together with I_{PA} , according to (2). A nearly δ_{crit} -periodicity with which the modes are changing can be seen in this figure. It shows that Δ_T is close to the total detuning difference Δ . The small deviation is due to electronic shift $\delta_n(x, z, N(z))$, which changes according to the changing carrier distribution $N(z)$ with increasing injection.

Black symbols in Fig. 4b) indicate the damping and the wavelength of four most important modes governing the dynamics of the laser, while tiny dashed curves show several other well damped modes. Red (grey) lines in the lower panel of this figure represent peaks in the simultaneously computed optical spectra of the emitted field. The laser operation at stationary state is indicated by the main spectral peak position coinciding with the wavelength of the dominant mode (lower panel) which has zero damping (upper panel). Close to the stability borders of the stationary state another low damped mode comes up. These modes start to interact with each other and perform mode-beating pulsations. This is characterized by the optical spectra with peak wavelength separation corresponding to the frequency separation of these two modes (lower panel). Since the change of electronic detuning with changing current is comparatively small, the experimentally observable basic red shift allows us to approximate the thermal detuning $\delta_{T,MO}$, while the periodicity of mode transitions give us information about detuning difference Δ_T and, thus, about $\delta_{T,PA}$ [4].

5 Conclusion

We have carried out theoretical and experimental investigations of the dynamics of monolithically integrated master-oscillator power-amplifier. The DFB laser acting as MO is designed for single longitudinal and lateral mode operation. Although the front facet of the PA is anti-reflection coated ($R \approx 10^{-3}$), both simulations and experiments and the above discussion show, that the MOPA works as a compound cavity device. This leads to dynamic instabilities, that are typical for multisection lasers, reported in [10], e.g.. The qualitative dynamic behavior strongly depends on temperature induced refractive index changes. The introduction of the self- and cross-heating model together with a mode analysis have allowed to achieve a good agreement of qualitative dynamic behavior between theory and simulations. We believe that our work provides a good basis for future study, and, in particular, provides some pointers for more detailed investigations of mechanisms behind the MOPA effects.

Acknowledgment

The work of M. Radziunas has been supported by DFG Research Center MATHEON.

References

- [1] Brien S.O., Lang R., Parke R., Welch D., and Mehuys D.: 2.2-W continuous wave diffraction-limited monolithically integrated master oscillator power amplifier at 854 nm. *IEEE Phot. Techn. Lett.*, **9**(4), 440–442 (1997)
- [2] Lammert R., Ungar J., Osowski M., Newkirk M., and Chaim N.: 980-nm master oscillator power amplifiers with non-absorbing mirrors. *IEEE Phot. Techn. Lett.* **11**(9), 1099–1101 (1999)
- [3] Wenzel H., Paschke K., Brox O., Bugge F., Fricke A.G.J., Knauer A., Ressel P., and Erbert G.: 10-W continuous-wave monolithically integrated master-oscillator power-amplifier. *Electron. Lett.* **43**(3), 160–161 (2007)
- [4] Spreemann M., Lichtner M., Radziunas M., Bandelow U., and Wenzel H.: Measurement and simulation of distributed-feedback tapered master-oscillators power-amplifiers. submitted to *IEEE J. Quant. Electron.* (2008)
- [5] Balsamo S., Sartori F. and Montrosset I.: Dynamic beam propagation method for flared semiconductor power amplifiers. *IEEE J. Quant. Electron.*, **2** (2), 378–384 (1996)
- [6] Egan A., Ning C.Z., Moloney J.V., Indik R.A., Wright M.W., Bossert D.J., and McInerney J.G.: Dynamic instabilities in master oscillator power amplifier semiconductor lasers. *IEEE J. Quant. Electron.*, **34**(1), 166–170 (1998)
- [7] Bandelow U., Radziunas M., Sieber J., and Wolfrum M.: Impact of gain dispersion on the spatio-temporal dynamics of multisection lasers. *IEEE J. Quant. Electron.* **37**(2), 183–188 (2001)
- [8] Lichtner M., Spreemann M.: Parallel simulation of high power semiconductor lasers. ser. WIAS Preprint. Berlin, Germany: WIAS, 2008, no. 1326. [Online]. Available: <http://www.wias-berlin.de/main/publications/wias-publ/>, to appear in Springer LNCS series
- [9] Radziunas M., Wünsche H.-J.: Multisection lasers: longitudinal modes and their dynamics. In: Piprek J. (ed.) *Optoelectronic Devices - Advanced Simulation and Analysis*, pp. 121–150. Springer, New York (2005)
- [10] Bauer S., Brox O., Kreissl J., Sartorius B., Radziunas M., Sieber J. Wünsche H.-J., and Henneberger F.: Nonlinear dynamics of semiconductor lasers with active optical feedback. *Phys. Rev. E* **69**(1), 016 206–016 215 (2004)
- [11] Tager A., Petermann K.: High-frequency oscillations and self-mode locking in short external-cavity laser diodes. *IEEE J. Quant. Electron.* **30**(7), 1553–1561 (1994)

- [12] Rehberg J., Wünsche H.-J., Bandelow U., and Wenzel H., Spectral properties of a system describing fast pulsating DFB lasers, *Z. angew. Math. Mech.* **77**(1), 75–77 (1997)